Adsorption (2008) 14: 525–532
DOI 10.1007/s10450-008-9131-z

Charge and discharge of methane on phenol-based carbon monolith

M.S. Balathanigaimani · Min-Joo Lee · Wang-Geun Shim · Jae-Wook Lee · Hee Moon

Received: 30 April 2007 / Revised: 21 January 2008 / Accepted: 18 April 2008 / Published online: 7 May 2008

Abstract Methane adsorptions on various synthesized and commercial activated carbons were assessed in a volumetric apparatus for the design of an efficient adsorbed natural gas storage system. Based on the methane adsorption equilibrium results from different carbon based materials, a monolith was also produced from RP-20. Dynamic studies were also performed for the prepared monolith and the pelletized commercial Norit-B4 activated carbon. The temperature variation in RP-20 monolith was analyzed and compared with those of Norit-B4 and a blank test, which consisted of a run without a sample. The temperature variation in RP-20 monolith was quite high compared to that observed with Norit-B4 and the blank test because of a higher isosteric heat of adsorption and a high packing density.

Keywords Activated carbons · Methane adsorption · Monolith · Dynamic studies

1 Introduction

Natural gas is one of the cleanest and abundant fuels which can substitute for gasoline in many aspects. Also natural gas is relatively inexpensive and one of the safest burning fuels. In spite of all the advantages, the energy density (the energy of combustion per unit volume) of natural gas is a drawback for effective utilization of natural gas. This is an important reason for designing of a separate storage system for natural gas. Disadvantages of the conventional storage methods such as liquefied natural gas (LNG) storage and compressed Natural Gas (CNG) storage have been discussed extensively in the literature (Biloe et al. 2001; Lozano-Castello et al. 2002; Menon and Komarneni 1998; Mota 1999). To overcome the problems inherent in the conventional methods, a newly upcoming adsorbed natural gas (ANG) storage system has been used for the natural gas storage. ANG is a method in which natural gas is stored by physisorption at 298 K and up to 35 atm. Because methane is the predominant constituent (about 90%) in natural gas, most of the researchers use methane for the preliminary studies of the ANG.

Success of an ANG process fully depends on the adsorbents characteristics. The activated carbon is a promising adsorbent which satisfies most of the requirements for the better design of an ANG vessel. Some activated carbons show low adsorption capacity on a volume basis (volume of methane adsorbed/volume of adsorbent) owing to their low packing density, even though their capacities are high on a mass basis (moles of methane adsorbed/grams of adsorbents). To solve this problem, the formation of monolith is an effective way of minimizing the void volume (Quinn and MacDonald 1992). With (Lozano-Castello et al. 2002) or without binder (Inomata et al. 2002), monoliths are being prepared for the ANG system.

The efficiency of an ANG system is influenced mainly by the heat and mass transfer properties as well as the microporous nature of the adsorbent (Chang and Talu 1996; Mota et al. 1997a).The exothermic and endothermic behaviors during the adsorption and desorption of methane

M.S. Balathanigaimani · M.-J. Lee · W.-G. Shim · H. Moon (✉)
Centre for Functional Nano Fine Chemicals and Faculty of Applied Chemical Engineering, Chonnam National University, Gwangju 500-757, South Korea
e-mail: hmoon@chonnam.ac.kr

J.-W. Lee
Department of Chemical and Biochemical Engineering, Chosun University, Gwangju 501-759, South Korea

largely cause the temperature variations in the dynamic operation (Biloe et al. 2002; Chang and Talu 1996; Mota et al. 1995, 1997b). The temperature changes during charge and discharge are also observed because of the heat transfer properties of an adsorbent bed, the heat exchange at the vessel wall and the mass transfer effect (Bastos-Neto et al. 2005; Mota et al. 1997a; Ridha et al. 2007). Ultimately, the temperature fluctuation during charge and discharge studies should be observed for a feasible designing of the ANG process.

In the present study, methane adsorption capacities of six different adsorbents were analyzed at 303.15 K and up to 35 atm in a volumetric apparatus. The six adsorbents included rice-husk activated carbon (AC-RH), phenol-based activated carbons such as AC-PKOH AC-PH_2O, RP-15 and RP-20 as well as Norit-B4. Based on the preliminary results, RP-20 was selected for the monolith preparation to enhance its methane adsorption capability on a volume basis. The RP-20 monolith was prepared by using poly vinyl alcohol (PVA) and poly vinyl pyrrolidone (PVP) binders. The charge and discharge ability of the prepared monolith as well as the heat and mass transfer effects were examined at 303.15 K and pressure up to 40 atm in a dynamic apparatus. Finally, the dynamic result of RP-20 monolith was compared with the blank test result as well as the dynamic result of a commercial Norit-B4 activated carbon to verify the heat effect.

2 Experimental

2.1 Sample preparation

2.1.1 Activated carbon

Activated carbons such as rice-husk activated carbon (AC-RH) and phenol-based activated carbons (AC-PKOH and AC-PH_2O) were synthesized in our laboratory. The recipes for the preparation of these activated carbons are available in our previous publication (Balathanigaimani et al. 2006). Various commercial activated carbons including RP-15, RP-20 (Kuraray Chemical Co., Ltd.,) and Norit-B4 (Norit Co.,) were also used in these investigations.

2.1.2 Monolith preparation

Poly vinyl alcohol (PVA) and poly vinyl pyrrolidone (PVP) binders were used for the preparation of monolith. Initially, 90 weight % of activated carbon (RP-20 powder) and 5 weight % of each binder were thoroughly mixed in water. Then the resultant mixture was completely dried and compressed at 5 MPa to make a monolithic form.

2.2 Adsorbent characterizations

Nitrogen sorption data were measured for all the adsorbents (excluding RP-15) and RP-20 monolith at 77 K using an automatic adsorption system (Micrometrics ASAP 2020 analyzer). The surface characteristics of samples RP-15 and RP-20 were analyzed by argon adsorption isotherms at 87 K using the same apparatus. The BET equation and the Horvath-Kawazoe (H-K) equation were employed for the calculations of the surface area and the micropore size distribution. The high resolution pictures of RP-20 powder and monolith form were captured by a field emission scanning microscope (FE-SEM) (S-4700 Hitachi Model).

2.3 Methane adsorption equilibrium studies

Methane adsorptions on various activated carbons and carbon monolith were performed in a volumetric apparatus. The detailed procedure and the schematic diagram of volumetric apparatus have been presented in our earlier research papers (Balathanigaimani et al. 2006; Lee et al. 2006, 2007).

2.4 Dynamic studies

Methane charge and discharge studies were conducted in a dynamic apparatus as shown in Fig. 1. Dynamic equipment is fully automatic and a cell (100 ± 1 ml) comprises its main part. The same amount of adsorbent (10 g) was used in all the experiments. All adsorbents were dried in a vacuum drier for 24 hr at 423.15 K before taken into the dynamic cell. A vacuum pump was connected with the apparatus for the removal of the impurities present in the adsorbent and in the cell. All charge studies were performed upto 40 atm at 303.15 K. Also the discharge processes were done upto 2 atm at 303.15 K. To give the isothermic condition, the dynamic cell was kept in a specially designed external vessel with hot water circulation. The temperature was observed by a K type thermocouple with a measurement range of ± 0.01 K, and the pressure was measured by a pressure transducer. Highly pure methane (99%) was used for this work to get a reliable result. The methane gas flow during charge and discharge was controlled by a mass flow controller (MFC). This system was completely controlled by a computer programme for easy operation and higher accuracy. The temperature, the pressure and the flow rate changes along with the time were recorded for each cycle separately. The discharged gas from each cycle was safely disposed through the ventilation line.

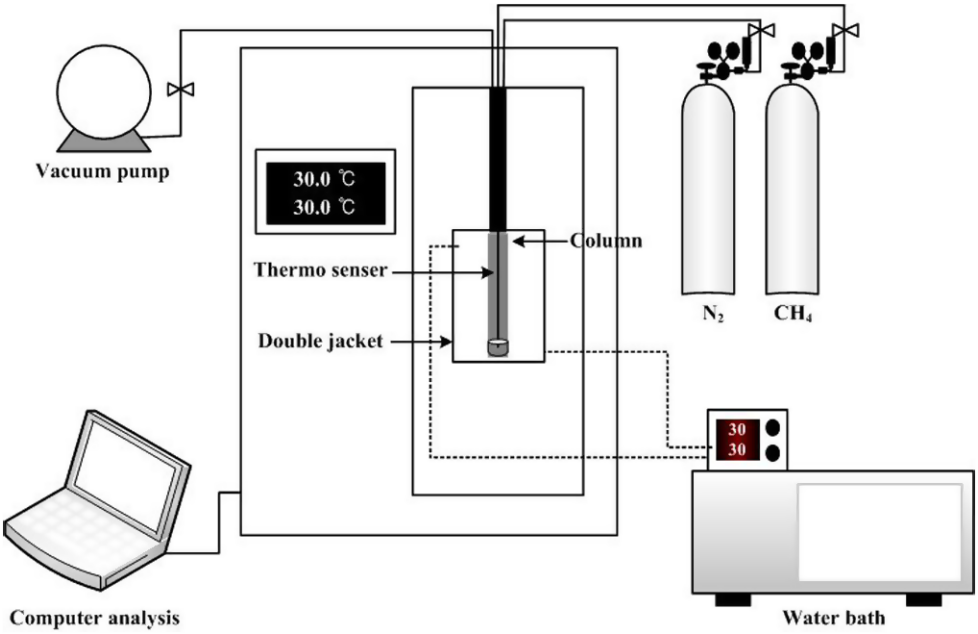

Fig. 1 Schematic diagram of dynamic apparatus

Table 1 Physical properties and methane adsorption capacities of various activated carbon samples

Activated carbon	BET surface area ($m^2 \cdot g^{-1}$)	Packing density ($g \cdot cm^{-3}$)	Micro pore volume (H-K) ($cm^3 \cdot g^{-1}$)	Methane adsorption on a mass basis† (mmol·g^{-1})	Methane adsorption on a volume basis† (V/V)
AC-RH	2350	0.056	0.746	9.40*	13*
AC-PKOH	2200	0.205	0.891	9.76	48
AC-PH_2O	1660	0.233	0.658	7.55	42
RP-15	1493[a]	0.220	0.449	6.59	3
RP-20	1853[a]	0.291	0.668	7.53	53
	1597				
Norit-B4	1170	0.430	0.450	5.01	52

†at 303.15 K and 35 atm

*at 303.15 K and 25 atm

[a]Argon adsorption

3 Result and discussion

3.1 Physical properties and morphologies of adsorbents

Nitrogen adsorption/desorption isotherms of AC-RH, AC-PKOH and AC-PH_2O have been presented in our previous paper (Balathanigaimani et al. 2006). Similarly, argon adsorption/desorption isotherms of RP-15 and RP-20 were shown in our previous report (Lee et al. 2007). The physical properties of all the activated carbon samples are given in Table 1. Nitrogen sorption data for powdered and monolith forms of RP-20 are shown in Fig. 2 together with the micropore distributions which were drawn on the basis of Horvath-Kawazoe (H-K) equation. Nitrogen adsorption isotherms of the two different samples showed type I characteristics defined by the International Union of Pure and Applied Chemistry (IUPAC) classification. The BET surface area, the micro pore volume and the density of these adsorbents are also given in Table 2 for better understanding.

The FE-SEM images of powdered and monolith forms of RP-20 are shown in Fig. 3a. These figures clearly show the large void volume in the powdered form in contrast to the monolithic form. Owing to the high compression pressure, the void volume was reduced in the monolithic form. The dimensions of monolith are clearly explained by using the photo images of monolith (Fig. 3b). The thickness and width of a monolith are 5 mm and 20 mm, respectively.

3.2 Methane adsorption capacity of various adsorbents

Methane adsorptions on adsorbents were done in a volumetric apparatus at 303.15 K and pressure up to 35 atm. Except for Norit-B4, methane adsorption isotherms of the other activated carbons have already been discussed in elsewhere (Balathanigaimani et al. 2006; Lee et al. 2007). In

Table 2 Comparison between the powdered and the monolith type of RP-20

Activated carbon	BET surface area ($m^2 \cdot g^{-1}$)	Packing density ($g \cdot cm^{-3}$)	Micro pore volume (H-K) ($cm^3 \cdot g^{-1}$)	Methane adsorption on a mass basis† ($mmol \cdot g^{-1}$)	Methane adsorption on a volume basis† (V/V)
RP-20 powder	1597	0.291	0.668	6.46	45
RP-20 monolith	1122	0.611	0.457	4.38	64

†at 303.15 K and 20 atm

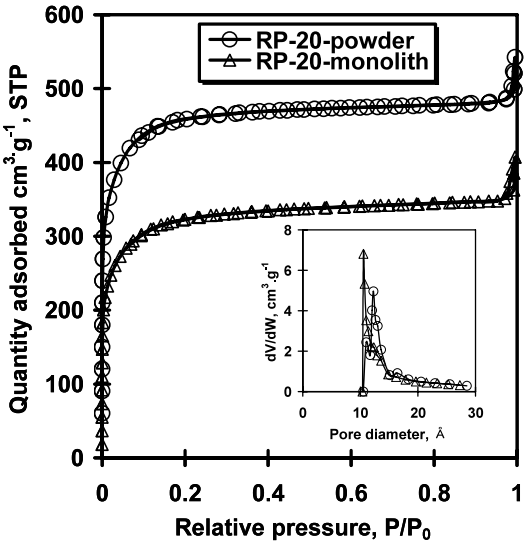

Fig. 2 Adsorption/desorption isotherms of nitrogen on powdered and monolith type of RP-20 and along with their H-K micropore size distributions

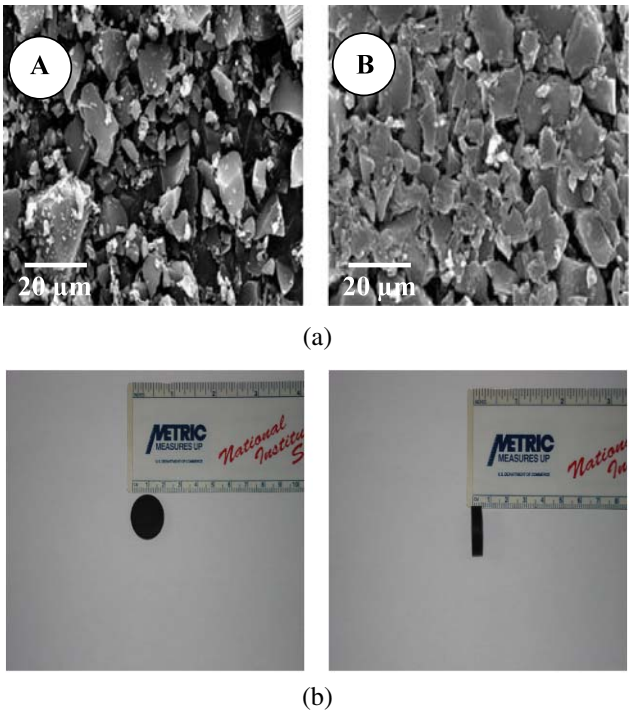

Fig. 3 FE-SEM pictures (powdered (A) and monolith (B) type of RP-20) (**a**), the dimensions of monolith (**b**)

this paper, the results of methane adsorption on all the activated carbon samples (including Norit-B4) were compared on a mass basis and also on a volume basis at 303.15 K as shown in Figs. 4a and b, respectively. On a mass basis, the high methane adsorption capacity was observed in AC-RH, followed by AC-PKOH, AC-PH_2O and RP-20. The large surface area of AC-RH is the reason for its high adsorption capacity on a mass basis. At the same time the capacity of AC-RH on a volume basis was very low compared to other adsorbents because of its low packing density. On a volume basis, RP-20 showed a high adsorption capacity contrast to other adsorbents because of its high packing density. Although the adsorption capacity of Norit-B4 was lower than RP-20 on a mass basis, its adsorption capacity on a volume basis was almost similar to RP-20 owing to its high packing density. The volumetric capacity of activated carbons could be increased through the reduction of void volume, and it was made possible by the monolith formation (Quinn and MacDonald 1992). Because of the high adsorption ability of RP-20 on a volume basis, RP-20 was chosen for the monolith preparation. The variation of isosteric heat of adsorption with respect to increasing adsorbed amount in RP-20 was almost constant compared to other adsorbents (Balathanigaimani et al. 2006; Lee et al. 2007), and this was also one of the reasons for the selection of RP-20 for the monolith preparation.

The packing density of RP-20 increased from 0.291 to 0.611 $g \cdot cm^{-3}$ and, of course, the increment in packing density is based on the quantity of binders and compression pressure. Simultaneously, the decrease in the surface area and in the average micropore size was observed with increasing packing density owing to the void volume reduction. Methane adsorption on prepared monolith was conducted at 303.15 K up to 23 atm in a volumetric apparatus similar to all other adsorbents. Methane adsorption values of powdered and monolith form of RP-20 were compared as shown in Fig. 4c. Compared to the powered RP-20 sample, the methane adsorption capacity of RP-20 monolith was low on a mass basis and high on a volume basis because of its low surface area and high packing density. On a volume basis, the adsorption capacity of powdered type RP-20 was about 53 V/V at 35 atm under 303.15 K, whereas it

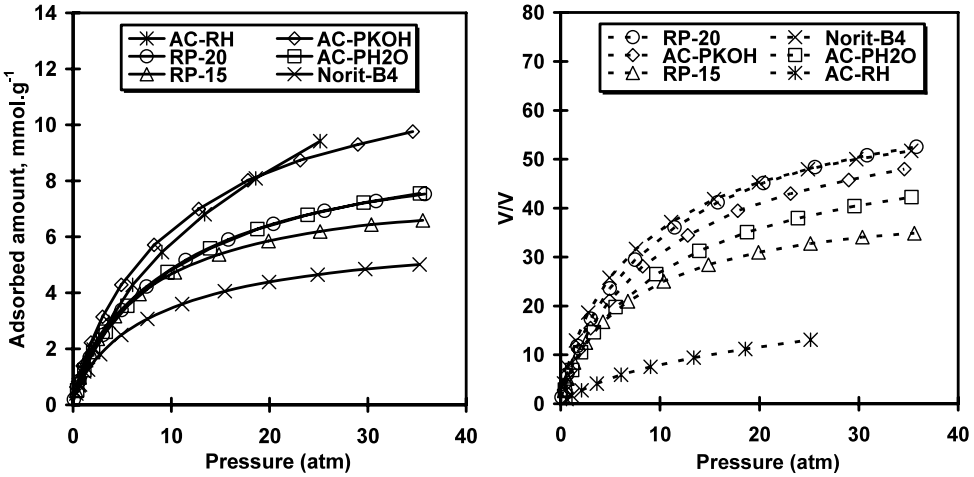

(a) (b)

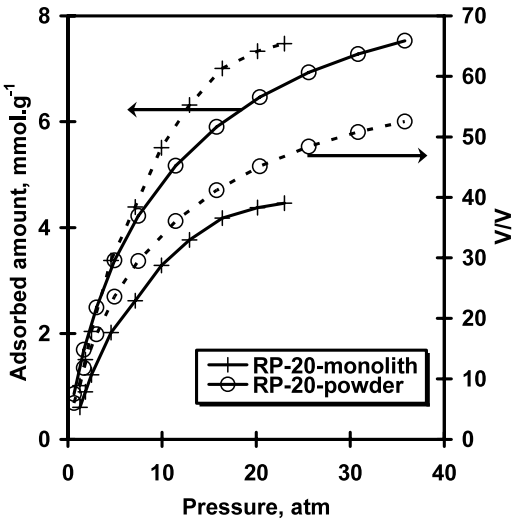

(c)

Fig. 4 Methane adsorption capacity of various activated carbons on a mass basis (**a**), Methane adsorption capacity of various activated carbons on a volume basis (**b**), Methane adsorption capacity of powdered and monolith type of RP-20 on a mass basis and volume basis (**c**)

was 65 V/V at 23 atm under 303.15 K for RP-20 monolith. It is interesting to note that the maximum adsorption capability of RP-20 powder at 303.15 K and 35 atm (53 V/V) could be achieved by RP-20 monolith within in 13 atm under 303.15 K. Table 2 lists the adsorption values of RP-20 powder and RP-20 monolith on a mass basis and volume basis at 303.15 K and 20 atm.

3.3 Methane charge and discharge studies

The cyclic operations of methane without adsorbent (blank test) and with adsorbents (RP-20 monolith and Norit-B4) were conducted for 10 cycles at 303.15 K and up to 40 atm for each run in a dynamic apparatus. For methane charge and discharge studies, the flow rate was fixed (90 ml/min) and controlled by a MFC. The blank test was performed to find out the exact temperature and pressure changes in a real dynamic study. Norit-B4 was also preferred for its pellet shape and high packing density. In this study, the temperature deviations in the prepared monolith (RP-20 monolith) are related with the results of commercial adsorbent (Norit-B4) and blank test to verify its capability. Also the stored amount, the amount of heat released during the charge and discharge as well as the amount of heat dissipated to the environment were calculated from these dynamic studies. The adsorbed amount $q_H - q_L$ during the charge study is calculated as follows:

$$\rho_b V(q_H - q_L) = \varepsilon V(C_L - C_H) + F_c t_c \tag{1}$$

where ρ_b is the packing density, V is the tank volume, ε is the interparticle porosity, F_c is the charge flow rate, t_c is the

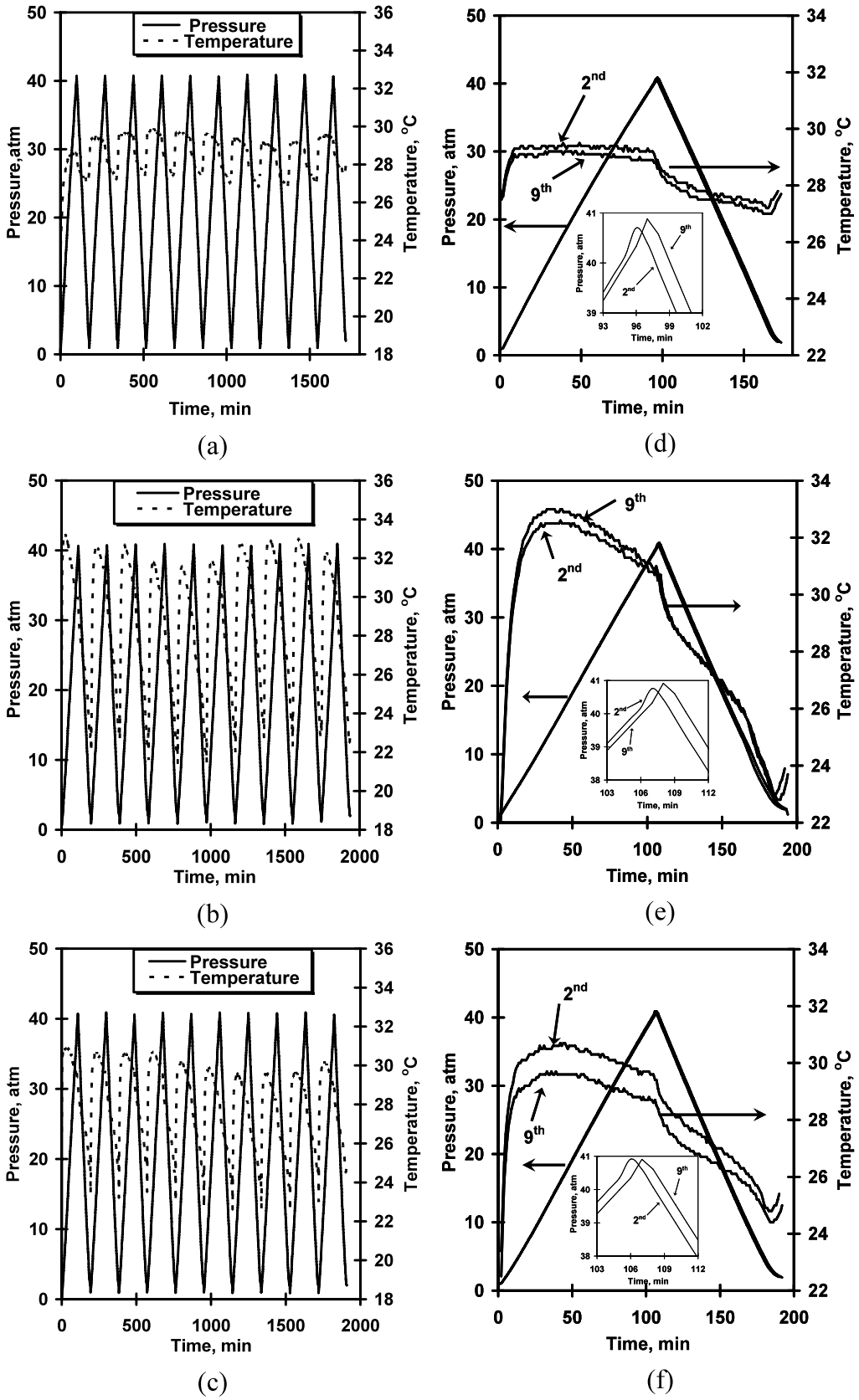

Fig. 5 The pressure and temperature variations during the dynamic operation ((**a**) Blank test, (**b**) RP-20 monolith and (**c**) Norit-B4). Comparison between the second and ninth cycle ((**d**) Blank test, (**e**) RP-20 monolith and (**f**) Norit-B4)

filling time, q is the amount adsorbed, and C is gas concentration at either depletion condition (L) or charge conditions (H). On the basis of the average value of the heat of adsorption obtained from the equilibrium study, the heat released during charge was estimated as $Q_s \rho_b V(q_H - q_L)$, where Q_s is the average value of the heat of adsorption. The amount of heat dissipated to the environment (Q_w) can easily be calculated using the simple energy balance equation as follows:

$$Q_s \rho_b V(q_H - q_L) = C_s \rho_b V(T_H - T_L) + Q_w \quad (2)$$

where C_s is the heat capacity of the adsorbent. In the case of RP-20 monolith, the calculated adsorbed amount, the amount of heat released, and the amount of heat dissipated to the environment were 5.81 mmol·g^{-1}, 7.81 kJ, and 7.73 kJ, respectively. The higher adsorbed amount (7.32 mmol·g^{-1}) and the lower heat released (4.14 kJ) as well as the lower heat dissipated to the environment (4.09 kJ) amounts were estimated from Norit-B4 compared to the monolithic form of RP-20.

Based on these cyclic results, the pressure and temperature variations along with time were plotted for each case as shown in Figs. 5a, b, and c. The temperature fluctuation range in the blank test was between 27° to 30°C, and it was very low compared to the dynamic tests with adsorbents. The temperature distribution ranges in RP-20 monolith and Norit-B4 were 21° to 33°C and 22° to 31°C, respectively. The isosteric heat of adsorption is one of the influencing parameters which affect the capacity of the storage system (Biloe et al. 2001). Although RP-20 has a relatively homogenous surface compared with Norit-B4, its isosteric heat of adsorption value (−19.88 to −20.31 kJ·mol^{-1}) (Lee et al. 2007) is higher than Norit-B4 (−6.83 to −16.57 kJ·mol^{-1}), and this might be attributed to the high temperature fluctuation in RP-20 monolith compared to Norit-B4.

The second and ninth cycle results of the blank test, RP-20 monolith and Norit-B4 were compared as shown in Figs. 5d, e, and f. In the blank test, the net temperature change was very low, and this change decreased from the second cycle to the ninth cycle along with a small increment in time. The same trend was observed in Norit-B4, but the only difference was the higher net temperature variations with higher temperature decrement from the second cycle to the ninth. In contrast to other two cases, the RP-20 monolith showed a totally different behavior. The higher range of net temperature distributions was seen in RP-20 monolith compared to the other two types. The temperature was slightly raised from the second cycle to the ninth cycle with a small time increment. The nature of the micropore size of the adsorbent also affects the capacity of the ANG system (Biloe et al. 2002; Pupier et al. 2005). The mean pore size difference between RP-20 monolith (14 Å) and Norit-B4 (32 Å)

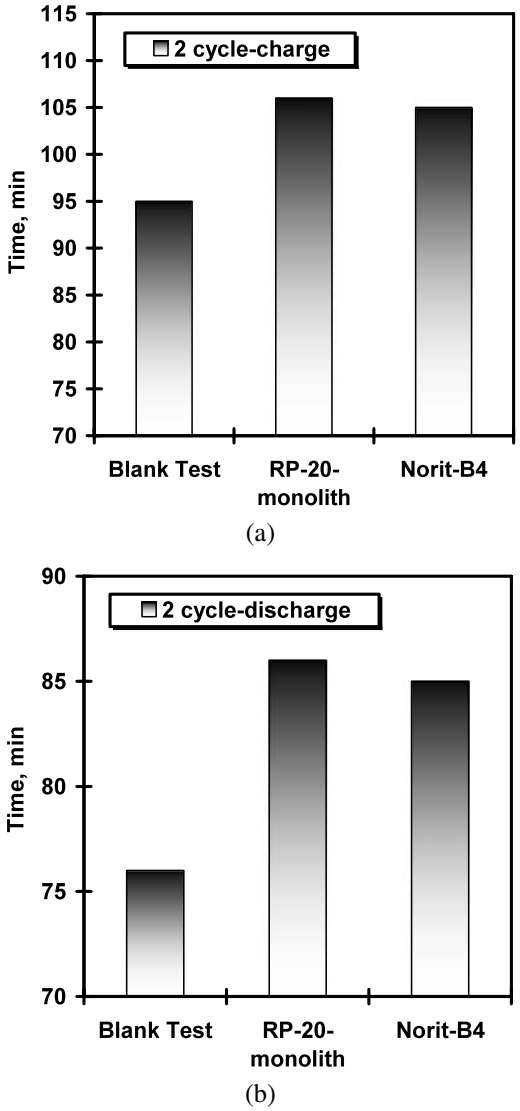

Fig. 6 The required time for the completion of the charge and discharge processes during the second cycle ((**a**) charge, (**b**) discharge)

and the isosteric heat of adsorption differences as discussed earlier are also the reasons for this high temperature fluctuation in RP-20 monolith.

The time required for charge and discharge in RP-20 monolith, Norit-B4 and blank test is compared. Particularly, the time required for the completion of the second cycle in each case was used for this analysis. This relationship is clearly shown for charge and discharge studies separately in Figs. 6a and b. The blank test showed less time requirement for both charge and discharge compared to the other two cases. A small time difference was observed between RP-20 monolith and Norit-B4 in both charge and discharge studies. The adsorption capacities of two adsorbents were observed from the time difference between the blank test and these two adsorbents.

4 Conclusions

Methane adsorption capacities of various activated carbons were evaluated at 303.15 K and up to 35 atm (except AC-RH) on a mass basis as well as on a volume basis. The powdered form of RP-20 activated carbon showed a high adsorption capacity on a volume basis among all the equilibrium studies. Monolith was prepared from RP-20 with the aid of polymeric binders to increase its packing density. The methane adsorption on RP-20 monolith was performed at 303.15 K up to 23 atm. The higher methane adsorption on a volume basis was observed in RP-20 monolith compared to the powdered form of RP-20. From the dynamic experiments, the higher temperature fluctuation was found in RP-20 monolith compared to other two cases because of its higher isosteric heat of adsorption and the lower micropore size.

Acknowledgement This work is supported by grant No. R01-2005-000-10742-0 from the Korea Science& Engineering Foundation.

References

Balathanigaimani, M.S., Kang, H.C., Shim, W.G., Kim, C., Lee, J.W., Moon, H.: Preparation of powdered activated carbon from rice husk and its methane adsorption properties. Korean J. Chem. Eng. **23**, 663–668 (2006)

Bastos-Neto, M., Torres, A.E., Azevedo, D.S., Cavalcante, C.L. Jr.: A theoretical and experimental study of charge and discharge cycles in a storage vessel for adsorbed natural gas. Adsorption **11**, 147–157 (2005)

Biloe, S., Goetz, V., Mauran, S.: Dynamic discharge and performance of a new adsorbent for natural gas storage. AIChE J. **47**(12), 2819–2830 (2001)

Biloe, S., Goetz, V., Guillot, A.: Optimal design of an activated carbon for an adsorbed natural gas storage system. Carbon **40**, 1295–1308 (2002)

Chang, K.J., Talu, O.: Behavior and performance of adsorpative natural gas storage cylinders during discharge. Appl. Therm. Eng. **16**(5), 359–374 (1996)

Inomata, K., Kanazawa, K., Urabe, Y., Ozono, H., Araki, T.: Natural gas storage in activated carbon pellets without a binder. Carbon **40**, 87–93 (2002)

Lee, J.W., Kang, H.C., Shim, W.G., Kim, C., Moon, H.: Methane adsorption on multi-walled carbon nanotube at (303.15, 313.15, and 323.15) K. J. Chem. Eng. Data **51**, 963–967 (2006)

Lee, J.W., Balathanigaimani, M.S., Kang, H.C., Shim, W.G., Kim, C., Moon, H.: Methane storage on phenol-based activated carbons at (293.15, 303.15, and 313.15) K. J. Chem. Eng. Data **52**, 66–70 (2007)

Lozano-Castello, D., Alcaniz-Monge, J., de la Casa-Lillo, M.A., Cazorla-Amorous, D., Linares-Solano, A.: Advances in the study of methane storage in porous carboneous materials. Fuel **81**(14), 1777–1803 (2002)

Menon, V.C., Komarneni, S.: Porous adsorbents for vehicular natural gas storage: a review. J. Porous Material **5**, 43–58 (1998)

Mota, J.P.B.: Impact of gas composition on natural gas storage by adsorption. AIChE J. **45**(5), 986–996 (1999)

Mota, J.P.B., Saatdjin, E., Tondeur, D., Rodrigues, A.E.: A simulation model of a high-capacity methane adsorptive storage system. Adsorption **1**, 17–27 (1995)

Mota, J.P.B., Saatdjin, E., Tondeur, D., Rodrigues, A.E.: Charge dynamics of a methane adsorption storage system: intraparticle diffusional effects. Adsorption **1**, 117–125 (1997a)

Mota, J.P.B., Rodrigues, A.E., Saatdjin, E., Tondeur, D.: Dynamics of natural gas adsorption storage systems employing activated carbon. Carbon **35**, 1259–1270 (1997b)

Pupier, O., Goetz, V., Fiscal, R.: Effect of cycling operations on an adsorbed natural gas storage. Chem. Eng. Process. **44**, 71–79 (2005)

Quinn, D.F., MacDonald, J.A.: Natural gas storage. Carbon **30**(7), 1097–1103 (1992)

Ridha, F.N., Yunus, R.M., Rashid, M., Ismail, A.F.: Thermal transient behavior of an ANG storage during dynamic discharge phase at room temperature. Appl. Therm. Eng. **27**, 55–62 (2007)